AC absorption and resistivity in the mixed state of highly anisotropic HTSC

M. A. Skvortsov and V. B. Geshkenbein

Landau Institute for Theoretical Physics of Russian Academy of Science, 142432 Chernogolovka, Moscow region, Russia

(Submitted 30 September 1993)
Zh. Eksp. Teor. Fiz. **105**, 1379–1395 (May 1994)

A theory of the skin effect in a sample with strong geometrical and electric anisotropy is developed. The results are applied to an analysis of recent experimental data on AC absorption peaks in the mixed state of highly anisotropic high temperature superconductors. These peaks are shown to be accounted for by a thermally activated resistivity behavior with an energy barrier $U(B) \propto \ln(H_{c2}/B)$.

1. INTRODUCTION

Recently a number of experiments on AC absorption in the mixed state of highly anisotropic high temperature superconductors were carried out, mechanical oscillator and AC response techniques being applied (see, for instance, Refs. 1 and 2). In these experiments, two peaks in the dissipation power were obtained. For a given sample, the position of the peaks depends[2] on the temperature T and DC magnetic field component B parallel to the c-axis of the superconductor. Various attempts were made to attribute these peaks to microscopic changes in vortex structure. In the paper,[3] however, it was argued that these peaks correspond to diffusion modes due to penetration of the field along different axis of the sample, and thus it is not necessary to invoke any phase transitions associated with these peaks.

It is essential that at the temperatures $T \ll T_c$ the peaks in AC absorption are situated in the region of thermally assisted flux flow (TAFF)[4] where electric resistivity is ohmic and exhibits Arrhenius dependence on temperature

$$\rho \propto \exp(-U(T,B)/T). \tag{1}$$

The ohmic nature of the resistivity allows us to propose the following scheme for the explanation of the two peaks.

At a given value of DC magnetic field B and temperature T, there exists an anisotropic resistivity tensor $\hat{\rho}=\mathrm{diag}(\rho_{ab},\rho_{ab},\rho_c)$ which in fact is due to microscopic behavior of vortices in TAFF regime. We are interested in the response of the sample to a small alternating magnetic field. As mentioned in,[5] this problem is analogous to that of AC magnetic field penetration into a normal metal. (The metal can be considered nonmagnetic, since for fields $B \gg H_{c1}$, the magnetic permeability $\mu \simeq 1$.)

We argue that the dissipation peaks have nothing to do with vortex phase transitions, but correspond to the maxima of dissipation due to eddy currents. These peaks can appear to be very sharp due to the exponential dependence of resistivity on temperature (1).

In analyzing the behavior of a conductor in the magnetic field $\mathbf{H}_a\exp(-i\omega t)$, it is convenient to introduce the field penetration depth

$$\delta=\sqrt{\frac{\rho c^2}{2\pi\omega}}, \tag{2}$$

which determines how deep the field penetrates into the sample. The peak in the imaginary part of the magnetic susceptibility occurs when the penetration depth is of the order of the characteristic dimension of the body. Straightforward application of this simple criterion to real superconducting samples is complicated by virtue of (i) large resistivity anisotropy $\gamma^2=\rho_c/\rho_{ab} \gg 1$, and (ii) slab geometry of samples (usually the ratio of dimensions of the sample along the c-axis and in the ab-plane is $\epsilon \ll 1$). The former implies that one should be careful in what ρ to substitute into the definition of δ, and the latter poses a problem as to what is the characteristic length to be compared with δ.

In the present paper these problems are solved; the results of the solution may appear useful in interpreting experimental data on linear AC response and mechanical oscillator measurements.

Let us consider a superconducting slab with dimensions along the c-axis and in the ab-plane equal to $a\epsilon$ and a respectively, $\epsilon \ll 1$. With the skin depth (2) determined via resistivity ρ_{ab}, the maximum in dissipation power happens when

$$\delta \sim \begin{cases} a\epsilon^{1/2} & \text{if } \mathbf{H}_a \parallel c; \\ a\epsilon & \text{if } \mathbf{H}_a \perp c, \quad \epsilon \ll \gamma^{-1}; \\ a\gamma^{-1} & \text{if } \mathbf{H}_a \perp c, \quad \gamma^{-1} \ll \epsilon. \end{cases} \tag{3}$$

These results were applied to analyze experimental data on linear AC response in order to extract values of electric resistivity from these indirect measurements. Values of ρ obtained in this way are in good agreement with recent experiments on resistivity.

On analyzing experiments of this type, it was found that in TAFF regime the resistivity obeys the Arrhenius dependence on temperature (1) with the activation barrier $U \propto U_0 \ln(H_0/B)$. Several formulas with this dependence $U(B)$ appeared elsewhere, but only the theoretical prediction in[6] is in reasonable agreement with the values found for U_0 and H_0. This gives extra support to the idea that the resistivity in TAFF regime is due to the motion of thermally activated dislocation pairs in a vortex lattice, and raises the problem of accurate estimation of the activation barrier for such motion.

 1063-7761/94/050743-08$10.00

2. SKIN EFFECT IN SLAB SAMPLES

In this section we consider a conductor in an external magnetic field $\mathbf{H}_a \exp(-i\omega t)$. We are interested in the case in which the conductor is a slab, i.e., its dimension $a\epsilon$ along the c-axis is much smaller than the dimension a in the ab-plane. The resistivity of the sample is a tensor $\hat{\rho}=\mathrm{diag}(\rho_{ab},\rho_{ab},\rho_c)$, where $\gamma^2=\rho_c/\rho_{ab}\gg 1$. In this geometry there are two essentially different situations. One of them corresponds to the field $\mathbf{H}_a \| c$, and the other to the field $\mathbf{H}_a \perp c$. Both of them will be discussed.

The skin effect in conductors is governed by the Maxwell equations, which for the case of an alternating field of frequency ω and ohmic resistivity can be written in the form

$$\mathrm{rot}\,\mathbf{E}=i\frac{\omega}{c}\mathbf{H}, \quad \mathrm{rot}\,\mathbf{H}=\frac{4\pi}{c}\hat{\sigma}\mathbf{E}, \tag{4}$$

where $\hat{\sigma}$ is the conductivity tensor, which vanishes in vacuum.

If the magnetic permeability of the body is $\mu=1$, the boundary condition at the conductor surface Γ takes the form

$$\mathbf{H}^{in}|_\Gamma=\mathbf{H}^{ex}|_\Gamma, \tag{5}$$

where indices "*in*" and "*ex*" designate the field inside and outside the sample. Far from the sample there is only external field $\mathbf{H}_a$:

$$\mathbf{H}(r\to\infty)=\mathbf{H}_a. \tag{6}$$

The system of equations (4)–(6) constitutes the problem to be solved.

We'd like to remind some general features of skin effect.[7]

The skin depth δ defined in (2) determines the length scale at which the field penetrates into the sample.

If δ is smaller than all characteristic dimensions of the body, including its smallest radius of curvature, then the field penetrates into the conductor in a thin layer of thickness $\delta\propto\omega^{-1/2}$ and thus at high frequencies full dissipation due to eddy current is proportional to $\omega^{-1/2}$. The standard method of calculating χ'' involves the computation of dissipation rate by means of integration of time averaged Poynting vector over the surface of the sample

$$Q=\frac{c}{4\pi}\oint\overline{\mathbf{E}\times\mathbf{H}}d\mathbf{f}, \tag{7}$$

and using the relation between Q and χ''

$$Q=\tfrac{1}{2}V\omega\chi''H_a^2. \tag{8}$$

At high frequencies the field almost does not penetrate into the sample and the distribution of the magnetic field outside the sample coincides with that one of the static field around the superconductor of the same shape.[7]

In the opposite case of large δ the field completely penetrates into the sample and one can calculate Q by integration

$$Q=\int\overline{\mathbf{j}\mathbf{E}}dV, \tag{9}$$

$\mathbf{E}$ being determined by the equation

$$\mathrm{rot}\,\mathbf{E}=i\frac{\omega}{c}\mathbf{H}_a. \tag{10}$$

In this case χ'' appears to be proportional to ω.

If the sample has the only characteristic dimension a then no third regime exists and the crossover between these two occurs when $\delta\sim a$. This corresponds to the peak in χ''.

This is not the case for a very compressed sample at $\mathbf{H}_a \| c$. We will show that in this situation the other regime with $\chi''\propto\omega^{-1}$ appears.

From mathematical point of view we have to find the continuous field $\mathbf{H}$, satisfying Laplace equation outside the sample and Helmholtz one inside. Generally speaking, this problem cannot be solved analytically for an arbitrary geometry.

The slab geometry we are going to discuss allows to eliminate some difficulties. First of all, in configurations with $\mathbf{H}_a \| c$ in effectively $2D$ (see subsection 2.1 below) or spheroid (subsection 2.2) geometry it is more convenient to work with electric field rather than with magnetic one because it is possible to choose the coordinate system where $\mathbf{E}$ has only one component E with respect to it. Then the mathematical problem is reduced to the following. There are Laplace-like operator L^{ex} outside the sample and Helmholtz-like L^{in} inside. We are looking for the continuous function E, satisfying $L^{ex}E=0$ in vacuum and $L^{in}E=0$ in the body, having continuous normal derivative on the surface and corresponding to constant magnetic field at infinity.

The slab geometry of the sample helps to solve the inner problem. With given value of $E|_\Gamma$ on the surface one can treat Helmholtz-like equation $L^{in}E=0$ in adiabatic way, considering the derivatives along the c axis as large and thus neglecting derivatives in ab plane. (This treatment has its roots in analogy between equation $L^{in}E=0$ and the Schrodinger equation for quantum motion inside the space bounded by the sample surface in which one can consider the motion along c axis as fast in comparison with slow one in ab plane.) The procedure discussed allows to express E in the bulk of the sample via the value of E on its surface. The solution of the inner problem being known, one can find its normal derivative on the surface and get boundary conditions for external problem. Thus using the slab geometry it is possible to reduce the solving of two coupled equations to one equation for the field outside the sample with the appropriate boundary condition. This external problem is to be solved by means of eigenfunctions of the operator L^{ex} or somehow else.

2.1. $H_a \| c$ skin effect in slab

Let us consider the sample occupying the volume $-a<x<a$, $-a\epsilon<y<a\epsilon$, $-\infty<z<\infty$ with the axes x,y,z being chosen along a,c,b crystallographic directions respectively. The applied ac field $\mathbf{H}_a$ has the only component along the $y(c)$ axis.

From the symmetry consideration it is evident that the electric field $\mathbf{E}$ (as well as the current $\mathbf{j}$ in the sample) is directed along the z axis. Thus the relation between $\mathbf{E}$ and

$\mathbf{j}$ is determined only by ρ_{ab} and is independent of the resistivity anisotropy γ. One can rewrite the system (4)–(6) in terms of $E=\mathbf{E}_z$:

$$\left(\frac{\partial^2}{\partial x^2}+\frac{\partial^2}{\partial y^2}+\frac{4\pi i\omega}{\rho c^2}\right)E^{in}=0, \quad \left(\frac{\partial^2}{\partial x^2}+\frac{\partial^2}{\partial y^2}\right)E^{ex}=0, \quad (11)$$

$$E^{in}|_\Gamma=E^{ex}|_\Gamma, \quad \left.\frac{\partial E^{in}}{\partial \mathbf{n}}\right|_\Gamma=\left.\frac{\partial E^{ex}}{\partial \mathbf{n}}\right|_\Gamma, \quad (12)$$

$$E^{ex}(r\to\infty)=i\frac{\omega}{c}H_a x. \quad (13)$$

Now we are going to solve this $2D$ problem. More precisely, we are looking for imaginary part χ'' of magnetic susceptibility. The real one can be expressed via χ'' with the help of Kramers–Kronig relation.

At low $\omega\chi''$ can be calculated as described above. From Eq. (10) [cf. Eq. (13)] one obtains

$$j=i\frac{\omega}{\rho c}H_a x. \quad (14)$$

The dissipation rate over unit length along z direction is given by

$$Q=2a\epsilon\int_{-a}^{a}\frac{1}{2\rho}\left(\frac{\omega}{c}\right)^2 H_a^2 x^2 dx=\frac{2}{3}a^4\epsilon\frac{\omega^2}{\rho c^2}H_a^2. \quad (15)$$

Using Eq. (8) we get

$$\chi''=\frac{1}{3}\frac{\omega}{\rho c^2}a^2=\frac{1}{6\pi}\kappa^2, \quad (16)$$

where we introduced a convenient quantity

$$\kappa=\frac{a}{\delta}. \quad (17)$$

The result (16) is valid until the magnetic field produced by the current flowing in the sample is smaller than H_a; only in this region it is possible to use the expression (14). The field produced by the current can be calculated according to Biot and Savart's law. In the middle of the slab one gets

$$H'=2a\epsilon\int_{-a}^{a}\frac{2}{c}\frac{j(x)}{x}dx=\frac{4i}{\pi}H_a\kappa^2\epsilon. \quad (18)$$

This means that the region of applicability of (16) is extended up to $\kappa\sim\epsilon^{-1/2}$.

The computation of χ'' at high frequencies (large κ) can be proceeded as follows. Let us suppose we know the electric field $E|_\Gamma$ on the surface of the sample and try to find the solution of the inner problem. We can treat Eq. (11) in a kind of adiabatic manner (see above) and write

$$E^{in}(x,y)=E(x,a\epsilon)\frac{\mathrm{ch}[(1-i)\kappa y/a]}{\mathrm{ch}[(1-i)\kappa\epsilon]}. \quad (19)$$

This approximation is correct while one can neglect x derivative in (11) in comparison with y one. We will consider the validity of adiabatic treatment (19) later in the section.

The inner problem being solved, one can obtain the boundary condition on E for the external problem. Taking the normal derivative of Eq. (19) on the surface of the body we find

$$\left.\frac{\partial E}{\partial n}\right|_\Gamma=(1-i)\frac{\kappa}{a}\mathrm{th}[(1-i)\kappa\epsilon]E|_\Gamma. \quad (20)$$

Since the smallness of ϵ had been already used one may consider this boundary condition as being set on the segment $[-a,a]$ of the x-axis.

So the problem is to find harmonic function E^{ex} obeying (13) and (20). According to the theory of potential one can express E^{ex} via function μ defined on the segment $[-a,a]$:

$$E(x,y)=i\frac{\omega}{c}H_a\left(x+\frac{1}{\pi}\int_{-a}^{a}\mu(x')\ln\left|r-r'\right|dx'\right), \quad (21)$$

where $|r-r'|^2=(x-x')^2+y^2$. In terms of μ the boundary condition (20) can be rewritten as the integral equation

$$\mu(x)=(1-i)\frac{\kappa}{a}\mathrm{th}[(1-i)\kappa\epsilon]\left(x+\frac{1}{\pi}\int_{-a}^{a}\mu(x')\times\ln\left|r-r'\right|dx'\right). \quad (22)$$

At high frequencies $\kappa\gg\epsilon^{-1/2}$ numerical factor in this expression is large ($|\kappa\mathrm{th}[(1-i)\kappa\epsilon]|\gg 1$) and neglecting LHS one can easily find the solution

$$\mu_0(x)=\frac{x/a}{\sqrt{1-(x/a)^2}}, \quad (23)$$

which corresponds to electric and magnetic fields on the upper surface of Γ given by

$$E_0(x)=i\frac{\omega}{c}H_a\frac{1}{(1-i)\kappa\mathrm{th}[(1-i)\kappa\epsilon]}\frac{x}{\sqrt{1-(x/a)^2}}, \quad (24)$$

$$H_0(x)=H_a\frac{x/a}{\sqrt{1-(x/a)^2}}. \quad (25)$$

There are three factors that restrict the applicability of simple expression (23) in the vicinity of the slab edges: (i) breakdown of adiabatic treatment (19), (ii) impossibility of neglecting LHS in (22), and (iii) impossibility of neglecting the thickness of the sample near its edges. We consider these restrictions in sequence.

With the given $\mu_0(x)$ one can obtain that (19) is correct as

$$a-|x|\gg a/\kappa. \quad (26)$$

On analyzing (22) it can be shown that simple solution (23) is valid while

$$a-|x|\gg\begin{cases}a/\kappa^2\epsilon & \text{if } \epsilon^{-1/2}\ll\kappa\ll\epsilon^{-1};\\ a/\kappa & \text{if } \epsilon^{-1}\ll\kappa.\end{cases} \quad (27)$$

The boundary Γ can be considered as a segment $[-a,a]$ at

$$a-|x|\gg a\epsilon. \quad (28)$$

Performing the integration of the Poynting vector over the surface of the sample [cf. (7)] we get

$$Q=\frac{c}{8\pi}\frac{\omega a}{c}H_a^2\,\mathrm{Re}\left\{\frac{1}{(1+i)\kappa\mathrm{th}[(1-i)\kappa\epsilon]}\right\}4$$
$$\times\int_0^{a^*}\frac{(x/a)^2}{1-(x/a)^2}\,dx, \tag{29}$$

where according to (26)–(28) the cutoff of divergent integral is

$$a^*\simeq\begin{cases}a-a/\kappa^2\epsilon & \text{if } \epsilon^{-1/2}\ll\kappa\ll\epsilon^{-1};\\ a-a\epsilon & \text{if } \epsilon^{-1}\ll\kappa.\end{cases} \tag{30}$$

Calculating the integral to logarithmic accuracy we find for $\epsilon^{-1/2}\ll\kappa\ll\epsilon^{-1}$

$$\chi''=\frac{1}{16\pi}\frac{\ln\kappa^2\epsilon}{\kappa^2\epsilon^2}, \tag{31}$$

and for $\epsilon^{-1}\ll\kappa$

$$\chi''=\frac{1}{16\pi}\frac{\ln 1/\epsilon}{\kappa\epsilon}. \tag{32}$$

Summarizing, we may write

$$\chi''=\begin{cases}\dfrac{1}{6\pi}\kappa^2 & \text{if } \kappa\ll\epsilon^{-1/2};\\ \dfrac{1}{16\pi}\dfrac{\ln\kappa^2\epsilon}{\kappa^2\epsilon^2} & \text{if } \epsilon^{-1/2}\ll\kappa\ll\epsilon^{-1};\\ \dfrac{1}{16\pi}\dfrac{\ln 1/\epsilon}{\kappa\epsilon} & \text{if } \epsilon^{-1}\ll\kappa.\end{cases} \tag{33}$$

2.2. $H_a\|$ c skin effect in oblate spheroid

We consider now the behavior of a conducting spheroid in alternating magnetic field. Let us choose axes x,y,z along a,b,c crystallographic axes of the sample. The bulk of the ellipsoid is bounded by the surface

$$\frac{x^2+y^2}{a^2(1+\epsilon^2)}+\frac{z^2}{(a\epsilon)^2}=1. \tag{34}$$

We again discuss the sample with $\epsilon\ll1$. The largest semiaxis of the spheroid is $a(1+\epsilon^2)^{1/2}\simeq a$, according to this definition a is the distance between the center of the spheroid and the focus of the ellipse in xz section. The problem is to get the solution of (4)–(6).

As one deals with spheroid geometry it is convenient to introduce the coordinates σ,τ,ϕ of oblate spheroid

$$x=a\sqrt{(1+\sigma^2)(1-\tau^2)}\cos\phi,$$
$$y=a\sqrt{(1+\sigma^2)(1-\tau^2)}\sin\phi, \tag{35}$$
$$z=a\sigma\tau.$$

This is an orthogonal system, the element of length is given by

$$dl^2=g_\sigma d\sigma^2+g_\tau d\tau^2+g_\phi d\phi^2; \tag{36}$$

$$g_\sigma=a^2\frac{\sigma^2+\tau^2}{1+\sigma^2},\quad g_\tau=a^2\frac{\sigma^2+\tau^2}{1-\tau^2},$$

$$g_\phi=a^2(1+\sigma^2)(1-\tau^2). \tag{37}$$

The introduced coordinates vary in the regions $0\leqslant\sigma<\infty$, $-1\leqslant\tau\leqslant1$, $0\leqslant\phi<2\pi$; relation $\sigma=\epsilon$ corresponds to the boundary of the spheroid.

Our purpose is to calculate χ'' as a function of the value κ defined by (17).

For low frequencies this calculation is analogous to the one described in the previous subsection and one obtains

$$Q=\frac{1}{2\rho}\int\mathbf{E}^2dV=\frac{\pi}{15}\frac{\omega^2}{\rho c^2}H_a^2a^5\epsilon(1+\epsilon^2). \tag{38}$$

Now from Eq. (8) we find that

$$\chi''=\frac{1}{20\pi}\left(\frac{a\sqrt{1+\epsilon^2}}{\delta}\right)^2. \tag{39}$$

This result is exact, it is valid for any oblate spheroid at sufficiently small κ. For $\epsilon\ll1$ one can estimate the magnetic field H' created by the current [cf. (18)] and find the criterion of applicability of this result by comparing H' and H_a. This had been already done in the similar situation in previous subsection and performing here the same estimation we come to the conclusion that for compressed spheroid (small ϵ) at $\kappa\ll\epsilon^{-1/2}$ χ'' is given by

$$\chi''=\frac{1}{20\pi}\kappa^2. \tag{40}$$

In the opposite case of high frequencies the magnetic field on the surface coincides with the field on the surface of the superconductor of the same form:

$$H_\tau|_{\sigma=\epsilon}=H_a\frac{\sin\theta}{1-n_z}, \tag{41}$$

where θ is angle between z axis and the external normal to ellipsoid at point (σ,τ,ϕ). n_z is z-component of demagnetizing tensor, for small ϵ $n_z\simeq1-\pi/2\epsilon$.

Performing the integration over the surface we find the rate of energy dissipation

$$Q=\frac{c}{16\pi}\sqrt{\frac{\omega\rho}{2\pi}}\oint H_\tau^2df$$
$$=\frac{c}{16\pi}\sqrt{\frac{\omega\rho}{2\pi}}\frac{H_a^2}{(1-n_z)^2}\int_{-1}^{1}2\pi\sqrt{g_\phi}\epsilon^2\frac{1-\tau^2}{\epsilon^2+\tau^2}\sqrt{g_\tau}d\tau$$
$$=\sqrt{\frac{\omega\rho}{2\pi}}\frac{ca^2\epsilon^2H_a^2}{4(1-n_z)^2}\sqrt{1+\epsilon^2}\left[\left(1+\frac{\epsilon^2}{2}\right)\ln\frac{1+\sqrt{1+\epsilon^2}}{\epsilon}\right.$$
$$\left.-\frac{\sqrt{1+\epsilon^2}}{2}\right]. \tag{42}$$

From here we get

$$\chi''=\frac{3}{8\pi}\frac{\delta}{a}\frac{1}{(1-n_z)^2}\frac{\epsilon}{\sqrt{1+\epsilon^2}}\left[\left(1+\frac{\epsilon^2}{2}\right)\ln\frac{1+\sqrt{1+\epsilon^2}}{\epsilon}-\frac{\sqrt{1+\epsilon^2}}{2}\right]. \tag{43}$$

For the case of the sphere of radius R $\epsilon=\infty$, $a\epsilon=R$, $n_z=1/3$ and from (43) we obtain a well known result[7] $\chi''=9/16\pi\delta/R$.

Our main interest is in compressed samples so we expand Eq. (43) and find at small ϵ

$$\chi''\simeq\frac{3}{2\pi^3}\frac{\ln 1/\epsilon}{\kappa\epsilon}. \tag{44}$$

Results (40) and (44) are rather trivial, they are obtained by means of standard perturbative approaches for low and high frequencies.

The way of obtaining χ'' at $\epsilon^{-1/2}\ll\kappa\ll\epsilon^{-1}$ is less transparent. As the problem of skin effect in slab was solved (see above), one would expect a similar behavior $\chi''\propto\omega^{-1}$ in the region in question.

It is convenient to introduce a new unknown function ψ, connected to electric field E by the condition

$$i\frac{\omega a}{2c}H_a\psi=\sqrt{(1+\sigma^2)(1-\tau^2)}E_\phi, \tag{45}$$

where E_ϕ is the only nonzero component of E in this coordinate system. Comparing with (37) we see that $\psi\propto rE_\phi$; ($r=\sqrt{x^2+y^2}$). If one excludes magnetic field from (4), the system (4), (5) can be rewritten in terms of ψ as follows

$$(1+\sigma^2)\frac{\partial^2\psi^{in}}{\partial\sigma^2}+(1-\tau^2)\frac{\partial^2\psi^{in}}{\partial\tau^2}+2i\kappa^2(\sigma^2+\tau^2)\psi^{in}=0, \tag{46}$$

$$(1+\sigma^2)\frac{\partial^2\psi^{ex}}{\partial\sigma^2}+(1-\tau^2)\frac{\partial^2\psi^{ex}}{\partial\tau^2}=0, \tag{47}$$

$$\psi^{in}|_\Gamma=\psi^{ex}|_\Gamma,\quad \left.\frac{\partial\psi^{in}}{\partial\sigma}\right|_\Gamma=\left.\frac{\partial\psi^{ex}}{\partial\sigma}\right|_\Gamma. \tag{48}$$

The scenario of solution of (46)–(48) was discussed in the beginning of this section. The inner problem will be solved in adiabatic way, whereas the outer one-by means of eigenfunctions of Eq. (47).

The function $\psi(\epsilon,\tau)$ on the boundary of the spheroid being known, one can find the solution of the inner problem using the smallness of ϵ and treating Eq. (46) in adiabatic approach. This means that we are looking for the solution of inner problem given by

$$\psi^{in}(\sigma,\tau)=\psi(\epsilon,\tau)\frac{\mathrm{ch}(\nu(\tau)\sigma)}{\mathrm{ch}(\nu(\tau)\epsilon)} \tag{49}$$

with function $\nu(\tau)$ to be determined. If $\kappa\epsilon\ll1$ then τ derivatives of *ch* in (49) can be neglected and we obtain by substituting (49) into (46)

$$\nu(\tau)=(1-i)\kappa\tau. \tag{50}$$

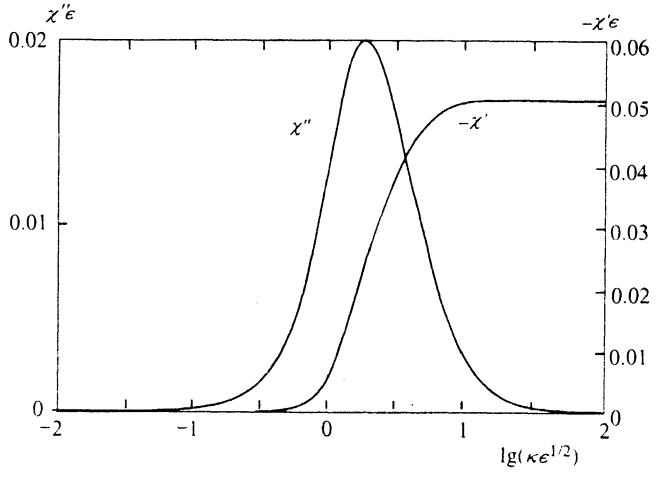

FIG. 1. Real (χ') and imaginary (χ'') parts of magnetic susceptibility of oblate spheroid (with axes ratio $\epsilon\ll10^4$). The maximum $\chi''_{\max}=0.0200\epsilon^{-1}$ at $\kappa=1.77\epsilon^{-1/2}$. Completely diamagnetic $\chi(\infty)=-1/2\pi^2\epsilon$.

Taking the derivative of (49) with this ν with respect to σ at the surface $\sigma=\epsilon$ one gets

$$\frac{\partial\psi(\epsilon,\tau)}{\partial\sigma}=\psi(\epsilon,\tau)\nu(\tau)\mathrm{th}(\nu(\tau)\epsilon), \tag{51}$$

and since $\kappa\ll\epsilon^{-1}$

$$\frac{\partial\psi(\epsilon,\tau)}{\partial\sigma}\simeq-2i\kappa^2\epsilon\tau^2\psi(\epsilon,\tau). \tag{52}$$

Equation (52) represents the boundary condition for the outer problem (47). It was reduced to the solution of the infinite system of linear equations on coefficients of expansion of ψ over eigenfunctions of Eq. (47) (see Appendix). This system was solved numerically in the region of $\kappa<\epsilon^{-1}$.

The results of computation are shown in Fig. 1. The dissipation maximum $\chi''_{\max}=0.0200\epsilon^{-1}$ occurs at $\kappa=1.77\epsilon^{-1/2}$. For $\kappa\ll\epsilon^{-1/2}$ χ'' is given by (40); for $\epsilon^{-1/2}\ll\kappa\ll\epsilon^{-1}$

$$\chi''=\frac{0.335}{\kappa^2\epsilon^2}. \tag{53}$$

The ratio $\chi''_{\max}/|\chi'(\infty)|=0.395$.

2.3. $H_a\perp c$ skin effect in oblate elliptical cylinder

Finally, let us consider the situation of an oblate elliptical cylinder with the axis y parallel to the axis of the cylinder, the bulk of the body is bounded by the surface

$$\frac{x^2}{a^2}+\frac{y^2}{a^2\epsilon^2}=1,$$

z coincides with the c axis. The cylinder is immersed in alternating magnetic field directed along y axis, i.e. $\mathbf{H}_a\perp c$.

In the geometry considered the current in the sample has components both in *ab* plane and along the c axis. Thus in this case anisotropy γ will be significant.

At low frequencies it can be shown that the distribution of current in xz section is given by

$$j_x=\frac{i\omega H_a}{c\rho_z}\frac{z}{\epsilon^2+\gamma^{-2}};\quad j_z=-\frac{i\omega H_a}{c\rho_z}\frac{\epsilon^2 x}{\epsilon^2+\gamma^{-2}}. \tag{54}$$

The calculation of the mean dissipation gives

$$Q=\int \overline{\mathbf{jE}}dxdz=\frac{\pi}{8}\frac{\omega^2 H_a^2 a^4}{c^2\rho_x}\frac{\epsilon^3\gamma^{-2}}{\epsilon^2+\gamma^{-2}}, \tag{55}$$

and we obtain

$$\chi''=\frac{1}{8\pi}\left(\frac{a}{\delta}\right)^2\frac{\epsilon^2\gamma^{-2}}{\epsilon^2+\gamma^{-2}}. \tag{56}$$

Here δ is determined via resistivity $\rho_x\equiv\rho_{ab}$.

The usual way of computation at high frequencies when penetration depth is small is to consider the surface as locally flat and use the expression for dissipation power at a flat surface. In this case we do the same, but first it is necessary to discuss the penetration of the field H_y into the semispace $x\sin\theta+z\cos\theta<0$. The resistivity in xz plane is anisotropic. It can be easily shown that the calculation of total dissipation can proceed in the conventional way for skin effect at high frequencies, but one should substitute resistivity ρ in formulas by the quantity

$$\rho(\theta)=\rho_x(\cos^2\theta+\gamma^2\sin^2\theta), \tag{57}$$

θ being the angle between the normal to the surface and the z axis. Performing the standard integration we obtain the dissipation per unit length in y direction

$$Q=\frac{c}{16\pi}\sqrt{\frac{\omega\rho_x}{2\pi}}H_a^2\oint\sqrt{\cos^2\theta+\gamma^2\sin\theta}dl. \tag{58}$$

Proceeding from integration over the boundary of the ellipse dl to integration over θ and using (8) one finds

$$\chi''=\frac{1}{2\pi^2}\frac{\delta}{a\epsilon^2}\int_0^{\pi/2}\frac{(\cos^2\theta+\gamma^2\sin^2\theta)^{1/2}}{(\cos^2\theta+\epsilon^{-2}\sin^2\theta)^{3/2}}d\theta. \tag{59}$$

Expressions (56) and (59) take simple form in two limit cases.

If $\epsilon\ll\gamma^{-1}$ then

$$\chi''=\begin{cases}\dfrac{1}{8\pi}\kappa^2\epsilon^2 & \text{if } \kappa\ll\epsilon^{-1};\\ \dfrac{1}{2\pi^2}\dfrac{1}{\kappa\epsilon} & \text{if } \epsilon^{-1}\ll\kappa.\end{cases}$$

If $\gamma^{-1}\ll\epsilon$ then

$$\chi''=\begin{cases}\dfrac{1}{8\pi}\kappa^2\gamma^{-2} & \text{if } \kappa\ll\gamma;\\ \dfrac{1}{6\pi^2}\dfrac{\gamma}{\kappa} & \text{if } \gamma\ll\kappa.\end{cases}$$

So we see that if geometrical compression is stronger than electric anisotropy $\epsilon\ll\gamma^{-1}$ then the peak in χ'' happens at $\delta\sim a\epsilon$; in the opposite case of strong electric anisotropy $\gamma^{-1}\ll\epsilon$ the peak occurs at $\delta\sim a\gamma^{-1}$. (Here δ is determined via ρ_{ab}.) This means that if anisotropy is strong enough then the effective compression of the sample in configuration $\mathbf{H}_a\perp c$ is determined by electrical anisotropy rather than geometrical dimensions.

3. APPLICATION TO THE ANALYSIS OF EXPERIMENTAL DATA

The results obtained in the previous section can be straightforwardly applied to analyze the experimental data on AC response and mechanical oscillator technique in TAFF regime. Within the point of view considered the existence and relative position of the two dissipation peaks usually detected in such types of experiments can get a simple and clear explanation. In these experiments it appears that for not too small angles between the external dc magnetic field and ab-plane of the sample, angles between the external dc magnetic field and ab-plane of the sample, the position of the peaks depends only on the temperature and the component B of the field parallel to the c-axis.[2] In interpreting such data, points where peaks occur are usually plotted in coordinates B,T. So, one gets two lines in B,T diagram, each corresponding to one of the peaks. The problem is how to interpret these lines.

Our point is the following. In TAFF regime at a given temperature and dc magnetic field the behavior of vortex structure gives rise to ohmic resistivity. Alternating magnetic field being applied to the sample, distinct absorption maxima appear due to the penetration of different components of the field into the sample. If the sample has a slab form then these maxima will be well separated. Certainly, the relative amplitudes of the peaks depend on the angle between the external alternating field $\mathbf{H}_a$ and the c-axis of the sample. In the two limit cases of $\mathbf{H}_a\parallel c$ and $\mathbf{H}_a\perp c$ only one peak is detected. The position of the peaks itself does not depend on the orientation of the ac field with respect to the sample and is determined by relations (3).

First we will analyze data of [2]. In this experiment double peaks in dissipation power were detected in ac response measurements performed on the crystal of BiSrCaCuO. Positions of the peaks were plotted on the diagram log B,T. We will discuss the TAFF region 20 K $<T<$ 50 K and 0.1 T $<B<$ 5 T of the diagram. Geometrical compression of the sample was $\epsilon=10^{-2}$.

Criterion (3) can be directly applied to $\mathbf{H}_a\parallel c$ case, whereas it is necessary to compare ϵ and γ^{-1} for a correct application of to $\mathbf{H}_a\perp c$ case. The paper [2] however does not supply us with the value of γ. An estimation of resistivity anisotropy can be extracted from the paper[8] where direct resistivity measurements were carried out on a similar BiSrCaCuO sample. This gives us a reasonable estimate $\gamma^2\sim 10^5$.

According to our result (3) this implies that one of the two curves corresponds to constant value of ρ_{ab} and the other to constant ρ_c, these values are given by

$$\rho_{ab}\simeq\frac{2\pi\omega}{c^2}a^2\epsilon \tag{60}$$

in configuration with $H_a\parallel c$, and

$$\rho_c \simeq \frac{2\pi\omega}{c^2} a^2 \tag{61}$$

in configuration with $H_a \perp c$.

Electrical anisotropy γ is certainly a function of B and T. But this dependence is negligible when compared to exponential dependence of resistivity on temperature. So we will take $\gamma^2(B,T)=\gamma_0^2=10^5$ in the region involved. This fact allows us to rewrite (61) in terms of ρ_{ab}

$$\rho_{ab} \simeq \frac{2\pi\omega}{c^2} a^2 \gamma_0^{-2}. \tag{62}$$

In the region considered one can clearly see that the lines of constant resistivities in [2] can be fitted with a high accuracy by straight lines in coordinates log B,T. Consequently, the activation barrier U in Arrhenius dependence (1) is logarithmically dependent on dc magnetic field B and the expression for ρ takes the form

$$\rho_{ab}=\rho_0 \exp\left(-\frac{U_0}{T}\ln\frac{H_0}{B}\right). \tag{63}$$

Thus we argue that the two lines in log B,T plane are lines of constant value of the same quantity ρ_{ab}. Taking into account (63), it can be the case only if the two straight lines, formally expanded to low temperatures, intersects at $T=0$. In the paper considered they really cross at $T=0$. This proves the correctness of our treatment and supplies the value of $H_0=200$ T. Now using formulae (60), (62) we can find two other unknown parameters in (63). The computation gives

$$\begin{aligned} &\rho_0 \simeq 10^4\ \mu\Omega\text{cm}; \\ &U_0 \simeq 100\ \text{K}; \\ &H_0 \simeq 200\ \text{T}. \end{aligned} \tag{64}$$

So, starting with the data of paper[2] and using our analytical results we obtained that the resistivity ρ_{ab} in the region considered obeys the relationship (63) with the set of parameters listed in (64), i.e. we managed to get resistivity from measurement of ac absorption.

It is interesting to compare this result with direct measurements of electric resistivity. Taking, for instance, the value of ρ_{ab} from [8] for $T=40$ K, $B=5$ T and comparing it with our result we find discrepancy by a factor of 2, which is negligible as compared with an overall scale of resistivity variations in the region considered.

There is another way to relate experimental data with the formula (63). It can be rewritten in the form

$$\rho_{ab}=\rho_0\left(\frac{B}{H_0}\right)^{U_0/T}. \tag{65}$$

So if a power dependence $\rho \propto B^{\alpha}$ at constant temperature T is detected in resistivity measurement experiment in TAFF regime then it follows that the parameter U_0 in (63) is given by $U_0=\alpha T$.

The values of α at different temperatures are $\alpha(40\ \text{K})=2.3$ (see [8]); $\alpha(33\ \text{K})=3.2$, $\alpha(20\ \text{K})=6$ (see [9]),

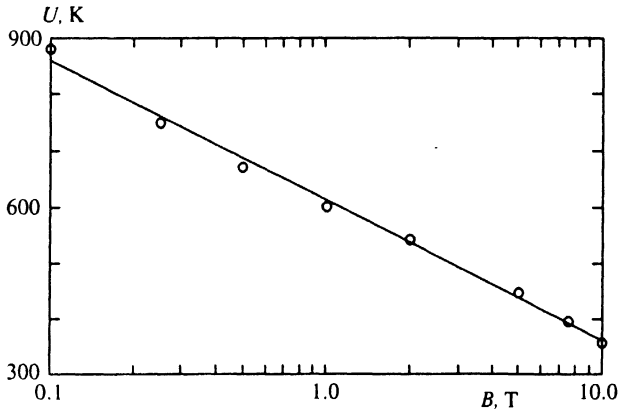

FIG. 2. Magnetic field dependence of the activation energy U of BiSrCaCuO. Data from [9] are replotted in coordinates log B,U.

which corresponds to the magnitude of the activation barrier of ~100, 100 and 120 K respectively and is in fine agreement with the values above.

The Eq. (63) describes the general behavior of resistivity in TAFF regime. Within our approach we can provide a new interpretation of the data obtained in [9]. In that paper log U was plotted as a function of log B and the authors obtained two regions with $U \propto B^{-1/6}$ at 0.1 T $< B <$ 3 T and $U \propto B^{-1/3}$ at 3 T $< B <$ 10 T. But if one plots the same graph in coordinates log B,U it will be clearly seen that the dependence is linear for all B considered (Fig. 2) and thus ρ_{ab} satisfies (63) with

$$\begin{aligned} &\rho_0 \simeq 10^5\ \mu\Omega\ \text{cm}; \\ &U_0 \simeq 100\ \text{K}; \\ &H_0 \simeq 400\ \text{T}. \end{aligned} \tag{66}$$

In the region discussed $T \sim 30$ K and dependencies (63) with the set of parameters (64) and (66) actually do not significantly differ from each other.

Finally, we'd like to mention the case of strong variation of resistivity anisotropy in narrow regions of temperature and field. At high magnetic fields and temperatures an effective Josephson coupling between superconducting layers can vary substantially with T and B,[10] thus leading to a steep variation of effective resistivity ρ_c. So it may appear for a slab sample that there exists a region where anisotropy drops from $\gamma^{-1} \ll \epsilon$ to $\gamma^{-1} \gg \epsilon$, which corresponds to the sudden increase of effective compression of the slab in configuration $\mathbf{H}_a \perp c$ [cf. (3)] and consequently to the drastic change in the position of ac absorption peak.

4. CONCLUSION

The two peaks in AC absorption in TAFF regime were discussed from the point of AC penetration into a normal metal with anisotropic resistivity. Criteria (3) were found, governing the position of the peaks in superconductors of slab geometry. Applied to the analysis of experimental data they allow to extract the value of resistivity corresponding

to the dissipation maxima from measurements of linear AC response or from mechanical oscillator experiments. It is shown that resistivities obtained in this way are in good agreement with direct resistivity measurements.

On analyzing resistivity data in TAFF regime it appeared that the resistivity obeys the general behavior given by (63) in the region in question.

Rigorous calculation of resistivity in TAFF regime is still not available, moreover there is no agreement in the nature of resistivity itself. Since parameters H_0 and U_0 in the activation barrier $U_0 \ln H_0/B$ appears to be close to the upper critical field H_{c2} (~ 100 T for BiSrCaCuO) and the energy scale of edge dislocations interaction $\epsilon_d \sim \Phi_0^2 d/64\pi^3\lambda^2$ (~ 60 K for BiSrCuCaO) respectively, we propose after [6] that the resistivity in TAFF regime is due to the thermally activated motion of dislocation pairs. The appearance of logarithm in the activation energy is originated in the interaction of vortex lattice with disorder [6]. The problem of accurate computation of activation barrier in this case is to be solved.

5. ACKNOWLEDGMENTS

We want to thank M. V. Feigel'man for numerous stimulating discussions, A. Larkin, Y. Yeshurun and E. Zeldov for their interest and useful comments; kind hospitality of the Physics Department of the Weizmann Institute of Science, where some part of this work was done, is greatly acknowledged.

APPENDIX

Here we present the solution of the outer problem (47), (19) with the condition at infinity $\psi(\sigma\to\infty;\tau)=(1+\sigma^2)(1-\tau^2)$, corresponding to the constant external field H_a, at $\kappa \ll \epsilon^{-1}$.

There are two types of eigenfunctions of (47)

$$\Psi_n = f_n(\tau)\Phi_n(\sigma); \quad \psi_n = f_n(\tau)\varphi_n(\sigma). \tag{67}$$

Φ_n grows as $\sigma\to\infty$, whereas φ_n vanishes at large σ. Explicit expressions for functions $f(\tau)$, $\Phi(\sigma)$ and $\varphi(\sigma)$ are listed below:

$$f_{2m}(\tau) = (-1)^m \frac{m!(m+1)!}{(2m)!(2m+1)!} \frac{\partial^{2m}(1-\tau^2)^{2m+1}}{\partial\tau^{2m}}, \tag{68}$$

$$\Phi_{2m}(\sigma) = \frac{m!(m+1)!}{(2m)!(2m+1)!} \frac{\partial^{2m}(1+\sigma^2)^{2m+1}}{\partial\sigma^{2m}}, \tag{69}$$

$$\varphi_{2m}(\sigma) = \Phi_{2m}(\sigma) \int_\sigma^\infty \frac{dx}{\Phi_{2m}^2(x)}. \tag{70}$$

Obviously, the choice of numerical coefficients in these definitions is somewhat arbitrary. As defined above, functions $f(\tau)$, $\Phi(\sigma)$, $\varphi(\sigma)$ satisfy the relations

$$f_{2m}(0)=1, \quad \Phi_{2m}(0)=1, \quad \varphi'_{2m}(0)=-1. \tag{71}$$

Function ψ as well as E accepts equal values at bottom and top semisurfaces of the spheroid. Thus, only even functions with respect to τ make contribution into expansion of ψ over eigenfunctions (67). Functions $f_n(\tau)$ with odd index n are odd, that's why we are not interested in them.

The magnetic field outside the sample may be viewed as consisting of two parts: external magnetic field H_a and induced H' which vanishes at infinity. So, the most general expansion of ψ over (67) takes the form

$$\psi(\sigma,\tau) = f_0(\tau)\Phi_0(\sigma) + \sum_{k=0}^{\infty} C_k f_{2k}(\tau)\varphi_{2k}(\sigma). \tag{72}$$

The problem is to find $\{C_k\}$.

Taking σ derivative of (72), equating it to the result (52) and substituting 0 for ϵ in arguments of function φ, one finds in the region considered

$$-\sum C_n f_{2n}(\tau) = -2i\kappa^2\epsilon\tau^2\left[f_0(\tau) + \sum C_n g_n f_{2n}(\tau)\right], \tag{73}$$

where

$$g_n = \varphi_{2n}(0) = \pi(2n+1)(n+1)\left[\frac{(2n)!}{n!(n+1)!2^{2n+1}}\right]^2. \tag{74}$$

Functions f_k are orthogonal with respect to scalar product

$$\langle f_{2k} f_{2n}\rangle \equiv \int_{-1}^{1} f_{2k}(x) f_{2n}(x) \frac{dx}{1-x^2} = 2^{4k+2} \frac{k!^2(k+1)!^2}{(k+1)(2k+1)(4k+3)(2k)!^2} \delta_{kn}. \tag{75}$$

Expanding (73) over f_{2n} with the help of (75) and auxiliary relations

$$\langle f_k \tau^2 f_{k-2}\rangle = -\frac{k^2-1}{4k^2-1}\langle f_k f_k\rangle, \tag{76}$$

$$\langle f_k \tau^2 f_k\rangle = \frac{2k^2+6k+1}{(2k+1)(2k+5)}\langle f_k f_k\rangle, \tag{77}$$

$$\langle f_k \tau^2 f_{k+2}\rangle = -\frac{(k+2)(k+4)}{(k+5)(k+7)}\langle f_k f_k\rangle, \tag{78}$$

one can get an infinite system of linear equations on coefficients C_k. The matrix of this system turns out to be tridiagonal. It was solved numerically.

[1] C. Duran *et al.*, Supercond. Sci. Technol. **5**, S272 (1992).
[2] J. Yazyi *et al.*, Physica (Amsterdam) **184C**, 254 (1991).
[3] E. H. Brandt, Phys. Rev. Lett. **68**, 3769 (1992).
[4] P. H. Kes *et al.*, Supercond. Sci. Technol. **1**, 242 (1989).
[5] V. B. Geshkenbein, V. M. Vinokur, and R. Fehrenbacher, Phys. Rev. B **43**, 3748 (1991).
[6] M. V. Feigel'man, V. B. Geshkenbein, and A. I. Larkin, Physica (Amsterdam) **167C**, 177 (1990).
[7] L. D. Landau, and E. M. Lifshitz, Electrodynamics of continuous media, Vol. 8 of *Course in Theoretical Physics*.
[8] R. Busch *et al.*, Phys. Rev. Lett. **69**, 522 (1992).
[9] T. T. M. Palstra *et al.*, Phys. Rev. Lett. **61**, 1662 (1988).
[10] L. I. Glazman, and A. E. Koshelev, Phys. Rev. B **43**, 2835 (1991).

This article was published in English in the original Russian journal. It is reproduced here with the stylistic changes by the Translation Editor.